# Synchronized concrete and bonding agent deposition system for interlayer bond strength enhancement in 3D concrete printing

Yiwei Weng, Mingyang Li*, Teck Neng Wong, Ming Jen Tan

Singapore Centre for 3D Printing, School of Mechanical and Aerospace Engineering, Nanyang Technological University, 50 Nanyang Avenue, Singapore, 639798

*Corresponding author: limingyang@ntu.edu.sg (M. Li)

## Abstract

A synchronized concrete and bonding agent deposition system is proposed to address the weak interlayer bond strength issue in extrusion-based 3D concrete printing (3DCP). In the proposed system, printable concrete and bonding agent are deposited concurrently via a rotatable nozzle with two outlets. Therefore, the interlayer bond strength is improved by the bonding agent deposited on the interface between printed filaments. Various bonding agents, including water, cement strengthener, polymer solution, and cement paste, were investigated. The results indicate that when the cement paste with a 0.26 water-to-cement mass ratio is adopted as the bonding agent, a relative bond strength as high as 267% can be obtained via the proposed system. Continuous printing was conducted to demonstrate that the proposed system has great potential for practical engineering applications. The proposed system has the potential to eliminate the weakness in interlayer bond strength of 3DCP processes and to widen 3DCP applications.

**Keywords**: 3D concrete printing; additive manufacturing; interlayer bond strength; synchronized system; bonding agent

## 1. Introduction

As a dominant technology in digital concrete, extrusion-based 3D concrete printing (3DCP) technique builds the structure by extruding materials layer-atop-layer through a digitally

controlled print-head. One of the main benefits of the 3DCP technology is that it can perform formwork-free concrete construction with enhanced design freedom without additional labor and cost [1–5]. Weng et al. [6] were the first in the area who conducted a quantitative comparison with firsthand data between a full-scale 3D printed prefabricated bathroom unit (PBU) and a precast PBU on economic values, environmental impacts, and productivity. Due to its formwork-free manufacturing, 3DCP outperforms the precast approach in small batches or customized PBU manufacture in all indexes [6].

However, a major hurdle to the wide adoption of extrusion-based 3DCP in the construction sector is the weak interlayer bond strength between printed filaments [7–11]. As will be reviewed in Section 2, the weak interlayer bond strength has a high correlation with the surface moisture content of printed filaments. The hydration between layers is impacted by the surface moisture content [7], which is affected by various factors. Among these factors, the interlayer time interval presents as a critical issue [12]. Various methods, including mechanical and chemical methods [13,14], have been proposed to improve the interlayer bond strength. However, at the current stage, all proposed methods for interlayer bond strength enhancement share one common and significant limitation - a lack of automation. The researchers either manually fabricated interlocking configurations by mold casting [13] or manually added polymer adhesives to the interface between layers [14], which would not be feasible for practical engineering applications. A detailed discussion of the limitations of the existing methods will be elaborated in Sections 2.3 and 2.4.

This work is mainly motivated by the limitation stated above. To address the lack of automation, a synchronized concrete and bonding agent deposition system for interlayer bond strength enhancement in 3DCP is proposed. This newly innovated system can deposit the bonding agent between the previous and new layers along with the concrete material printing process. Consequently, the interlayer bond strength can be improved by the bonding agent. In this work, the proposed system is also adopted in continuous printing to demonstrate its potential for practical engineering applications.

The proposed system for interlayer bond strength enhancement is challenging in several aspects. Firstly, an engineering-available solution should be adopted to apply the bonding agent evenly and effectively atop the printed filament surface. Secondly, the concrete printing process should not be obstructed by the bonding agent deposition process. Thirdly, the concrete

delivery speed and the bonding agent conveying speed should be coordinated to print the concrete and deposit the bonding agent in a synchronized manner. Finally, the adopted bonding agent should be effective in enhancing the interlayer bond strength.

The remainder of this article is organized as follows: In Section 2, the impact and origin of the weak interlayer bond strength in 3DCP are discussed, followed by a literature review on the existing methods to enhance the interlayer bond strength and the corresponding limitations. In Section 3, a novel print-head to perform the desired concurrent deposition process is illustrated, and its working mechanism is introduced. In Sections 4 and 5, the experiment design and results are presented and discussed. In Section 6, the presented work is summarized and discussed, and the future works are sketched.

## 2. Related works

In this section, the impact and origin of weak interlayer bond strength on 3D printed cementitious material properties are reviewed. Furthermore, the existing methods to address the weak interlayer bond strength issue are elaborated, and their corresponding limitations are discussed. Finally, a summary of this section is provided, and the research gap is identified and emphasized.

### 2.1. Anisotropic properties of printed material

Various 3D concrete printing materials have been developed in the past few years. Among all of the material properties, the anisotropic mechanical properties of 3D printed elements have been tested and reported in many studies [15–18]. Le et al. [15] first evaluated the hardened properties of high-performance printing concrete. In this study, the mold-cast specimens were investigated as control concrete with high strength (107 MPa in compression, 11 MPa in flexure, and 3 MPa in direct tension). However, the well-printed concrete specimens in the same study [15] had a compressive strength of 75 - 102 MPa, a flexural strength of 6 - 17 MPa, depending on testing direction, and direct tensile strengths between layers varying from 2.3 to 0.7 MPa, reducing as the interlayer time interval increased. Similar work was conducted by Wolfs et al.

[16], in which the bond strength between layers reduced as interlayer time intervals increased. The anisotropic phenomenon was also found in the geopolymer printing by Xia and colleague(s) [17,18].

In summary, these earlier works clearly showed that the weak interlayer bond strength of the printed concrete material results in strong anisotropic properties, which are mainly reflected by the mechanical performance of printed specimens. Apart from the mechanical properties, the acoustic indexes also reflected the anisotropic properties of 3D printed concrete [19].

## 2.2. Origins of weak interlayer bond strength

The surface moisture content is considered an essential parameter that impacts the interlayer bond strength. Sanjayan and Xia [20] investigated the impact of interlayer time interval on the interlayer bond strength of printed concrete, and a correlation was found between the interlayer bond strength and the surface moisture content at the interface between layers. Their work revealed that a higher surface moisture content achieves a better direct tensile strength between layers. The surface moisture content, in turn, depends on the bleeding rate of the concrete and the drying rate of moisture from the surface.

A similar finding was reported by Keita et al. [7], wherein a superficial extremely localized drying is at the origin of a drop in interlayer bond strength of flowable mortars with low water-to-cement mass ratio. Moreover, their findings suggest that the drying localization is formed because the liquid does not have time to flow and replace the evaporated liquid in low porosity fresh materials. Consequently, a dry region is expected to develop from the drying interface and to propagate in the sample. Without enough water to hydrate the cement powder in the dry region, the interlayer bond strength would decrease. Likewise, Wolfs et al. [16] quantitatively presented the strength reduction analysis, where approximately 33% - 50% reduction was reported for the specimens left uncovered for long time intervals of 4 h and 24 h. Additionally, the impact of surface moisture content on interlayer bond strength is also supported by findings outside the field of 3DCP [21].

## 2.3. Methods to enhance the interlayer bond strength

Methods to enhance the interlayer bond strength can be categorized based on various mechanisms, primarily mechanical and chemical ones. A typical mechanical method to enhance the interlayer bond strength is introduced by interlocking two adjacent layers. In the study by Zareiyan and Khoshnevis [13], a concrete mixture compatible with the extrusion system was used, and different mold configurations were introduced to test interlocking effects. Their findings revealed that the interlayer bond strength is sensitive to interlocking configurations, and the strength can be increased by an average of 26%, according to the tensile splitting test. The observed increase in interlayer bond strength could be attributed to the increase in the contact surface area between layers.

In terms of the chemical methods to enhance the interlayer bond strength, Hosseini et al. [14] adopted polymer adhesive as the bonding agent to enhance the interlayer bond strength, and their experiment results presented a considerable increase in the interlayer bond strength, which was characterized by 3-point bending test. The two-fold rise in interlayer bond strength and chemical cohesion proved that their method could enhance bonding between adjacent layers. Similar works and results were also presented by Wang et al. [22] and Marchment et al. [23].

## 2.4. Research gap

All the above-mentioned methods on interlayer bond strength enhancement share the same limitation - a lack of automation. The researchers either manually fabricated the interlocking configurations by mold casting or manually added the polymer adhesive to the interface between layers. Besides, a further concern is on the efficiency of the interlocking method on improving interlayer bond strength. While introducing polymer as the bonding agent can gain a two-fold rise in interlayer bond strength [14], the interlocking method could only achieve a 26% improvement in interlayer bond strength [13].

The research gap in automation and efficiency motivates this project on a synchronized concrete and bonding agent deposition system to enhance the interlayer bond strength. In the presented synchronized concrete and bonding agent deposition system, the printable concrete

and the bonding agent were delivered and deposited concurrently. As the concrete delivery speed and the bonding agent convey speed can be coordinated, the amount of deposited bonding agents atop the printed filament surface can be controlled without obstructing the concrete printing process. This system allows bonding agents to be automatically deposited on the interface between layers to enhance the interlayer bond strength efficiently.

## 3. Print-head design for the synchronized deposition system

### 3.1. Print-head design and deposition schemes

One of the main challenges to enhance the interlayer bond strength via the bonding agent is that a specific dosage of the bonding agent needs to be deposited automatically between layers without obstructing the concrete printing process. A possible method to achieve this target is to adopt multiple printing heads or printing devices. However, this method will result in redundant positioning sub-systems, the risk of end-effectors collision, and the misalignment of the concrete and the bonding agent. To avoid such disadvantages, a more intuitive and straightforward approach to achieving concurrent concrete and bonding agent deposition process is proposed in this work.

A novel print-head was designed to perform the desired concurrent concrete and bonding agent deposition process. This print-head is composed of a rotatable nozzle and a flow splitter fixed on the print arm, as shown in the computer-aided design (CAD) model in Fig. 1. The nozzle, which consists of a concrete outlet and a bonding agent outlet, is rotatable to keep the center plane of its two outlets aligned with the printing direction. The flow splitter uses two symmetric branches to balance the flow distance of the bonding agent and, thus, helps to maintain a stable flow rate. During the printing process, the bonding agent is delivered to the flow splitter, discharged into the funnel, which rotates with the nozzle, and then released from the bonding agent outlet, as shown by the dashed lines in Fig. 1. Simultaneously, the concrete is delivered to and extruded from the central outlet of the nozzle as in a typical 3DCP process. A longitudinal-section view along the symmetry plane of the nozzle, as well as the flow directions of the concrete material and the bonding agent, are shown in Fig. 2.

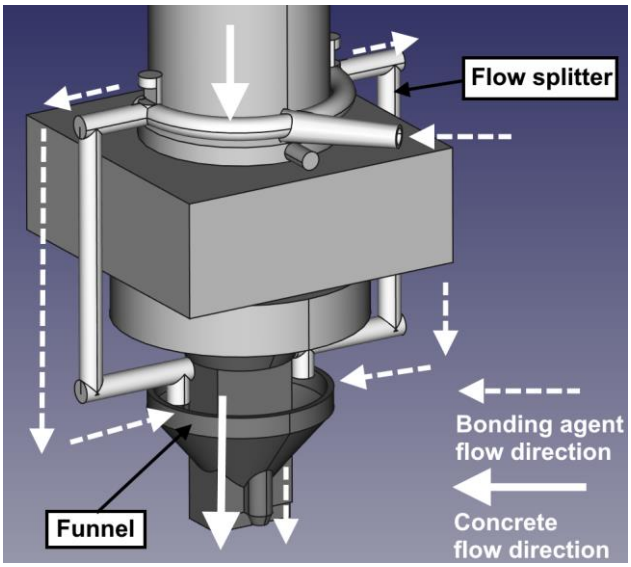


Fig. 1 The CAD model and delivery mechanism of the designed print-head.

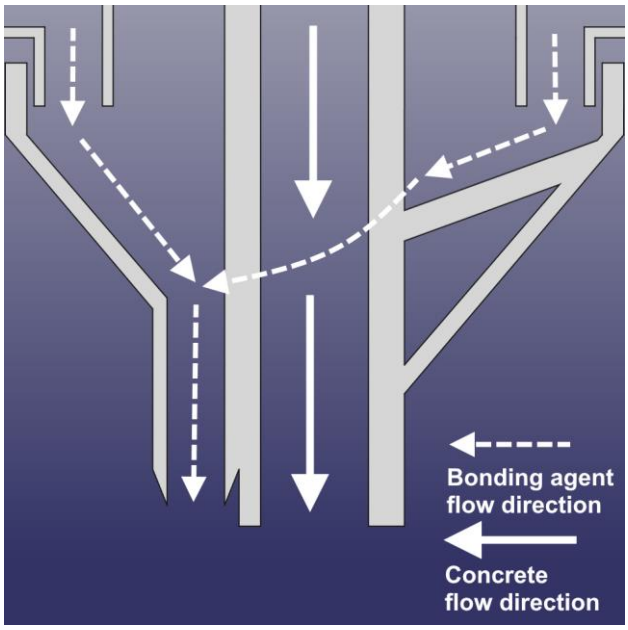


Fig. 2 The longitudinal-section view along the symmetry plane of the rotatable nozzle.

Two different deposition schemes, as shown in Fig. 3, were derived from the presented print-head design. In the first deposition scheme (Scheme 1; Fig. 3(a)), the bonding agent outlet is behind the concrete outlet, and the bonding agent is deposited on the top surface of the new concrete filament. With this deposition scheme, the bonding agent deposition position is only affected by the printing path radius of the new layer, and it can be properly applied atop of the concrete filament surface (except in some special situations, as will be discussed in Section 3.2). However, there is a time gap between the deposition of the bonding agent and the

extrusion of the next concrete layer, which may affect the bonding effect. In the second deposition scheme (Scheme 2; Fig. 3(b)), the bonding agent outlet is in front of the concrete outlet, and the bonding agent is deposited on the top surface of the previous concrete layer and immediately covered by the new concrete layer. However, if there is an offset between the new layer and the previous layer, the bonding agent may fall from the printed part and provide no bonding effect.

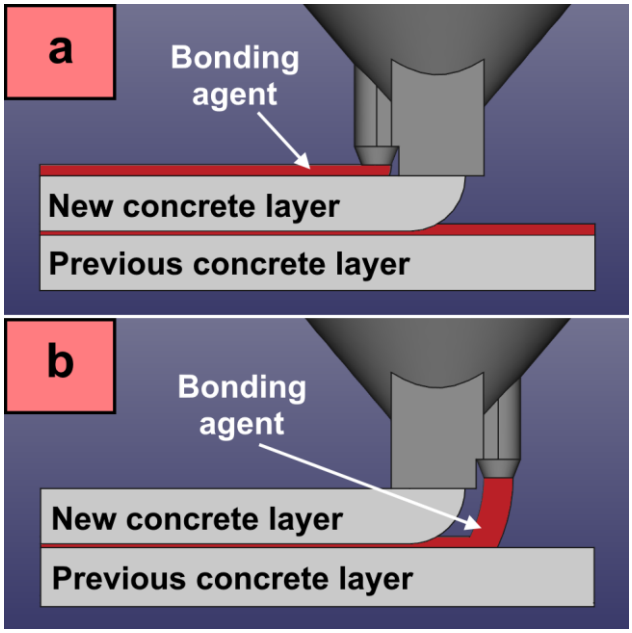


Fig. 3 The concurrent concrete and bonding agent deposition schemes: (a) The bonding agent outlet is behind the concrete outlet, and the bonding agent is deposited on the top surface of the new concrete layer; (b) The bonding agent outlet is before the concrete outlet, and the bonding agent is immediately covered by the bottom surface of the new concrete layer.

The suitability of the two printing schemes is determined by two factors - the bonding agent and the printing path. If the bonding agent needs some time to take effect, then Scheme 1 should be adopted to give a particular setting time for such a bonding agent. Conversely, if the effect of a bonding agent reduces and expires in a period of time shorter than the interlayer time interval, Scheme 2 should be adopted to maximize the effectiveness of such a bonding agent. Besides, if there is a large offset between the successive concrete layers, Scheme 1 should be adopted to offer a better chance to keep the bonding agent on the printed part.

### 3.2. Dealing with highly viscous bonding agents

Most of the bonding agents adopted in this work, including the cement strengthener, the polymer solution, and the cement paste, have a high viscosity, introducing additional design constraints for the presented system. Since the bonding agent is purely driven by gravity in the presented nozzle design, the size of the flow channel is important for the bonding agent to flow smoothly. While a flow channel with 4 mm hydraulic diameter is sufficient for water, a flow channel with a 6-8 mm hydraulic diameter is needed for the cement strengthener and the polymer solution to flow smoothly, and the flow channel for cement paste should have a hydraulic diameter no less than 15 mm.

However, the bonding agent flow channel size is not the larger the better. A large bonding agent flow channel may cause a position offset between the bonding agent and the concrete filament in a curved printing path. For example, as shown in Fig. 4, when a 30 mm × 15 mm nozzle (L × W) with 3 mm wall thickness is used in a 30 mm radius printing path, the centerline of the moving path of a 15 mm diameter bonding agent outlet has a 5 mm offset from the centerline of the printing path. Therefore, in the case where the printing path contains small radius curve sections, the bonding agent outlet needs to be reduced to avoid an unacceptable offset. To make the bonding agent flow smoothly in such a narrow flow channel, a hydraulic slip ring can be added to the system, and the bonding agent can be driven by the power of the bonding agent pump.

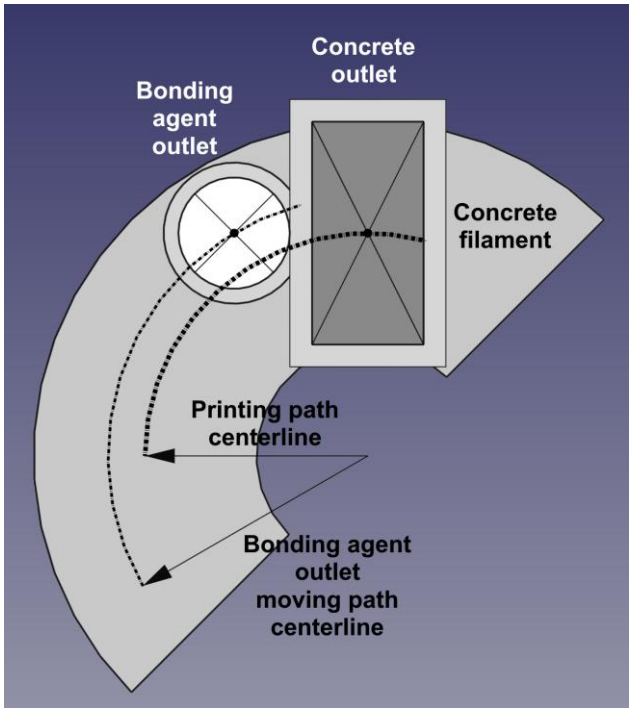

Fig. 4 The centerline of the bonding agent outlet moving path offsets from the centerline of a curved printing path.

The other problem is that the high viscosity of the bonding agent can obstruct the even distribution of the bonding agent on the interface. Although most of the bonding agents can be paved by the pressure of the next concrete filament, some tend to keep their shape and cause additional defects on the interface. To deal with this problem, bonding agent spreaders were designed to pave the highly viscous bonding agents in different deposition schemes, as shown in Fig. 5. For Scheme 1, where the bonding agent outlet is behind the concrete outlet, the spreader needs to be attached behind the bonding agent outlet (Fig. 5(a) and (b)); for Scheme 2, where the bonding agent outlet is in front of the concrete outlet, the spreader needs to be attached between the bonding agent outlet and the concrete outlet (Fig. 5(c) and (d)).

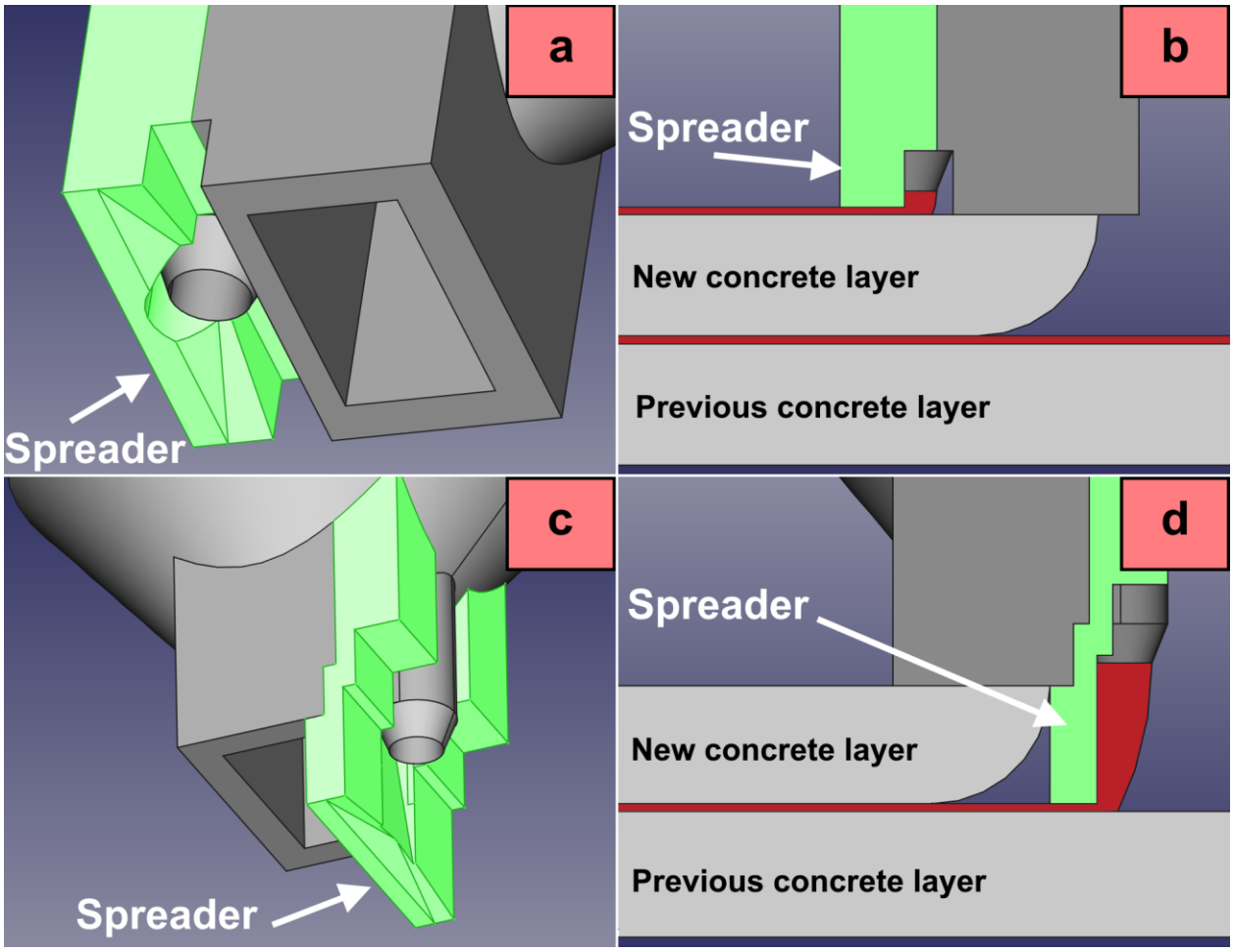


Fig. 5 The bonding agent spreaders and corresponding deposition schemes: (a) The CAD model of the spreader for Scheme 1; (b) The spreader for Scheme 1 paves the bonding agent atop the

new concrete layer; (c) The CAD model of the spreader for Scheme 2; (d) The spreader for Scheme 2 paves the bonding agent atop the previous concrete layer.

## 4. Materials and methods

### 4.1. 3D printable concrete mix and bonding agents

The concrete material adopted in this work was the 3D printable concrete mix used by Weng et al. [24]. The mix consists of ordinary Portland cement (OPC), fly ash, silica fume, silica sand, water, and polyvinyl alcohol (PVA) fiber. The physical and chemical properties of all raw ingredients are shown in [24]. The mix proportions are presented in Table 1.

Table 1 Mix proportions of the ingredients of the 3D printable concrete.

| OPC | Fly ash | Silica fume | Silica sand | Water | PVA fiber |
|---|---|---|---|---|---|
| 1.000 | 1.000 | 0.050 | 1.025 | 0.574 | 0.023 |

Note: The numbers are mass ratios of each ingredient to OPC.

In order to screen the effective bonding agents, several potential materials, including water, a cement strengthener, a polymer solution, and a cement paste, were investigated in this work. Water was adopted as the bonding agent since many studies indicated that the surface moisture content is associated with the interlayer bond strength, and, in general, a higher surface moisture content leads to better interlayer bond strength [7,20]. The cement strengthener (W1 Cement Strengthener, Warrior Pte Ltd.) was a commercialized chemical solution for improving bond strength between two substances, such as concrete and tiles. The polymer solution used in this work was made by dissolving the polymer powder (ETONIS® LL5999 – 8331, Wacker Pte Ltd) in the water at a polymer-to-water mass ratio of 1:4. The polymer powder is usually added to the cement mix to improve cohesive strength. The cement paste used in this work was mixed by a 0.26 water-to-cement mass ratio with the addition of superplasticizer. The cement was Type I ordinary Portland cement, and the superplasticizer (ADVA 181N, GCP Applied Technologies) was 0.35 wt.% of cement content.

## 4.2. Printing path design

The printing path design for investigating the effect of different bonding agents on the interlayer bond strength is plotted in Fig. 6. Various bonding agents, as indicated in Fig. 6, were applied atop the filament surface with Scheme 1, and a nozzle without a spreader was adopted. During the printing process, the initial layer was printed while the bonding agent was simultaneously deposited atop the printed concrete filament. After a time interval of 40 minutes, the second layer was printed atop the initial layer. The nozzle travel speed and concrete pump rotational speed were 4,000 mm/min and 650 rpm, respectively. The nozzle outlet for the concrete material printing was 30 mm × 15 mm (L × W) in size. During the deposition process of the bonding agents, the bonding agent deposited atop each printed filament surface was approximately 10 mL in volume, which is approximately 500 mL/m$^2$.

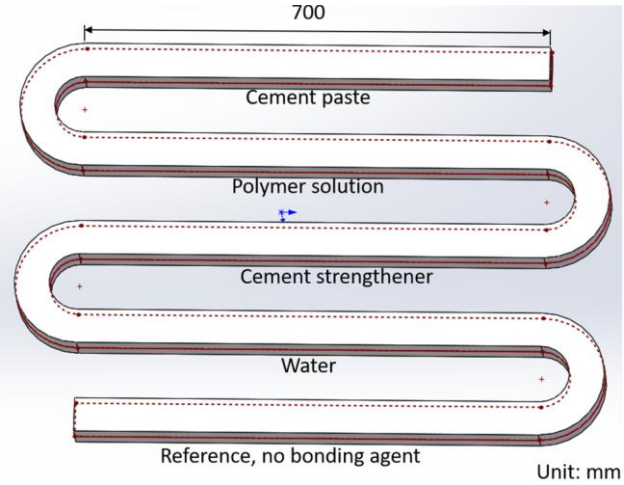


Fig. 6 The printing path design for investigating the effect of different bonding agents.

As discussed in Section 3.2, most of the bonding agents can be paved by the pressure of the next concrete layer; however, some may keep their formation and cause additional defects on the interface, which are detrimental to the interlayer bond strength. Therefore, to avoid the additional defects, a bonding agent spreader was adopted to pave the bonding agents. The printing path to study the impact of the spreader on the interlayer bond strength is shown in Fig. 7, where a different type of nozzle is adopted, i.e., a nozzle with a spreader. During this printing process, the initial layer was printed without depositing bonding agents. After a time interval of 40 minutes, the second layer was printed while simultaneously depositing the

cement paste atop the initial layer. The other experiment parameters were the same as in the printing shown in Fig. 6.

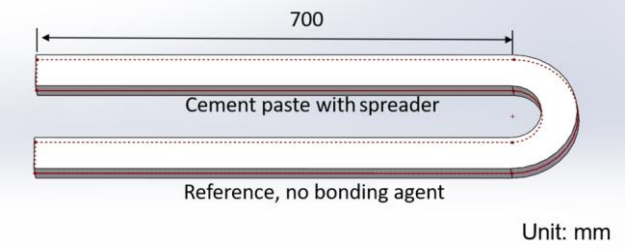


Fig. 7 The printing path design for investigating the effect of the bonding agent spreader.

### 4.3. Interlayer bond strength characterization

The interlayer bond strength was evaluated by the splitting tensile test according to ASTM C 496 [25], albeit in a scaled-down size to accommodate with the dimensions used in the 3DCP process [16,26,27]. The splitting tensile test was setup as depicted in Fig. 8. An Instron machine was used to apply the load with a loading rate of 0.1 mm/min. The splitting tensile tests were conducted after the printed filaments were cured for 7 days. The printed filaments were cut into small samples (50 mm in length) by a Struers Secotom-15 diamond cutter between days 2-6. At least three samples were prepared and tested for each bonding agent.

The interfacial splitting tensile strength is obtained via the following formula [26]:

$$f_t = \frac{2P_u}{\pi A}$$

where $f_t$ (MPa) is interfacial tensile splitting strength; $P_u$ (N) and $A$ (mm$^2$) are the ultimate load and the contact surface area between concrete filaments, respectively.

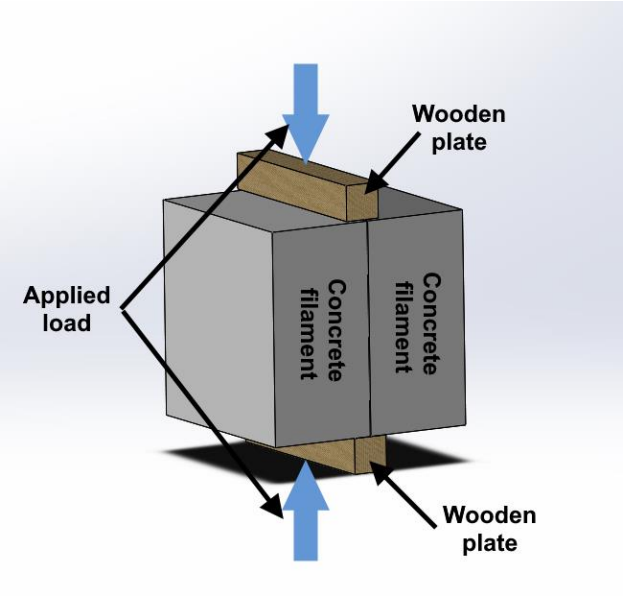


Fig. 8 The splitting tensile test setup.

## 5. Results and discussion

### 5.1. Printing system

The printing setup is shown in Fig. 9, where a concrete pump and a dosing pump were used to deliver the printable concrete material and the bonding agent, respectively. The concrete pump is illustrated in Fig. 10. During the concrete delivery process, the printable concrete material was poured into the material container, and was pushed by the material puncher into a delivery pump. A pressure gauge was installed on the delivery pump to measure the pumping pressure. The material puncher ensured that the concrete material could be delivered consistently, and the filament could be printed uniformly without discontinuity. A digital controller was installed on the concrete pump to control the pump rotational speed, and another digital controller was installed on the material puncher machine to control the punching frequency.

The dosing pump is shown in Fig. 11. During the bonding agent deposition process, the bonding agent was poured into the container, and its delivery speed was controlled by the digital controller. A flow meter (AXG002, Yokogawa Pte. Ltd) was used for measuring the flow rate of the bonding agent. Although the concrete pump and the dosing pump were working separately at the current stage, the entire system, including the concrete printer, the concrete

pump, and the dosing pump, can be integrated to achieve easier control of the printing, delivery, and deposition processes in the future.

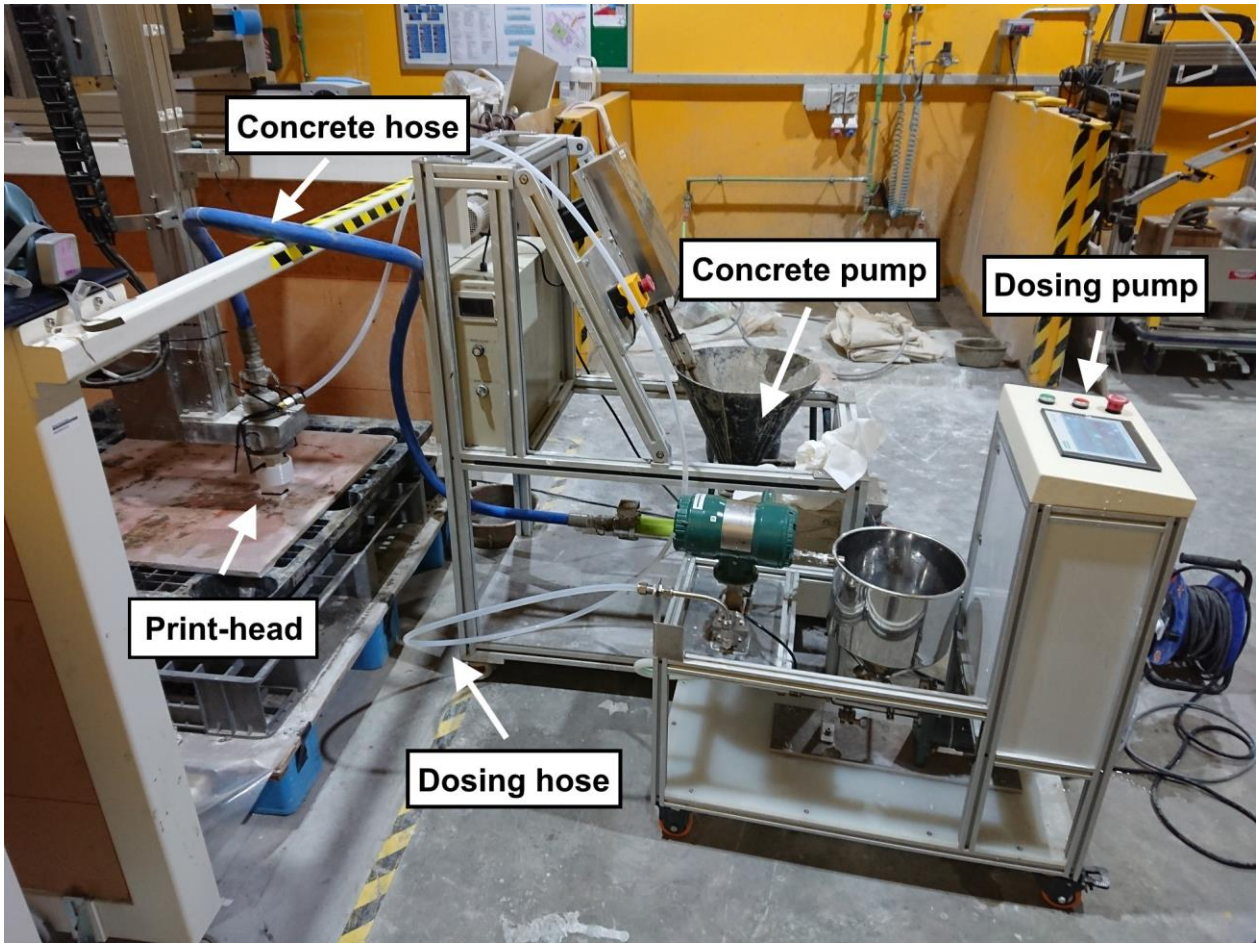


Fig. 9 The synchronized concrete and bonding agent deposition system.

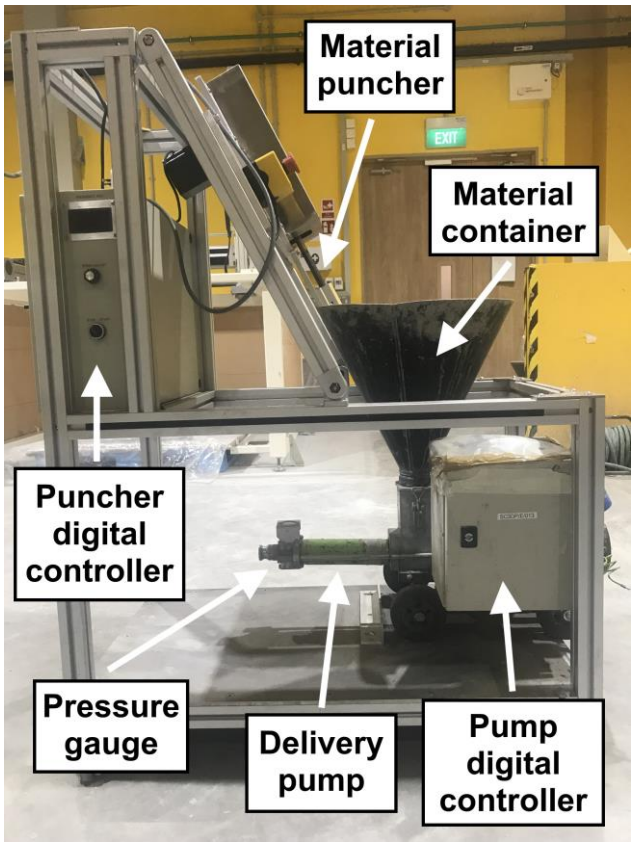


Fig. 10 The concrete pump.

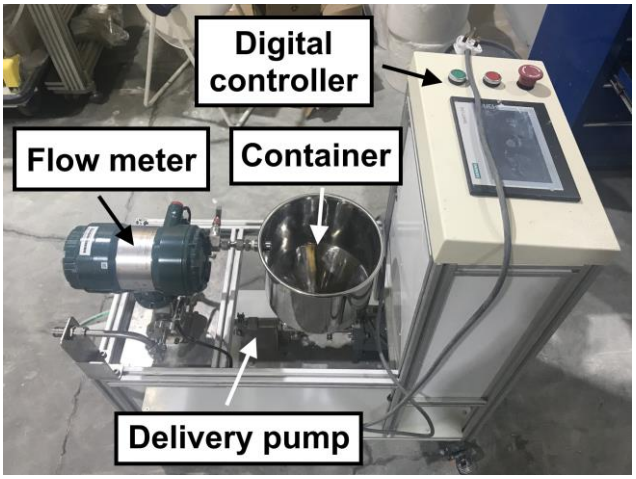


Fig. 11 The dosing pump for bonding agent delivery.

The prototype of the designed print-head, which was manufactured by a Raise3D Pro2 FDM 3D printer with polylactic acid, is shown in Fig. 12. Scheme1 in Fig. 3(a) was adopted in the printing path shown in Fig. 6 to study the effects of various bonding agents. As seen in Fig. 12, the delivery directions of the printable concrete material and the bonding agent are indicated

387 by the solid arrow line and the dash arrow lines, respectively. The funnel receives the bonding
388 agent and then delivers it to the bonding agent outlet, as shown in Fig. 13.
389

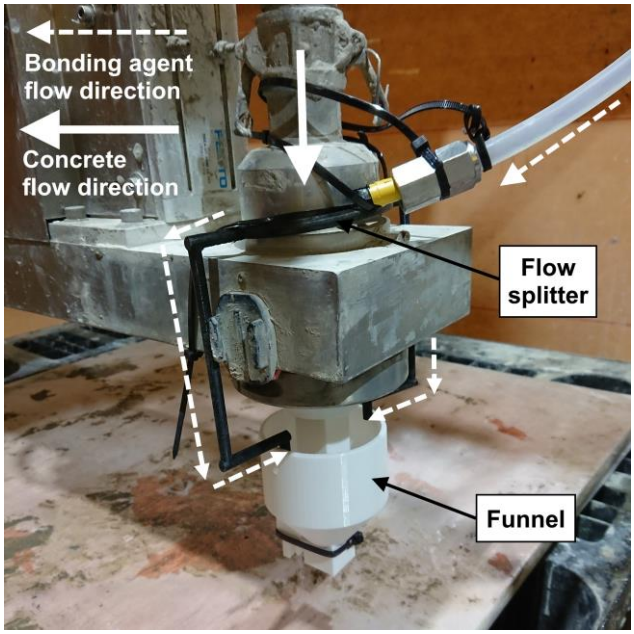


390
391 Fig. 12 The prototype of the proposed print-head.
392

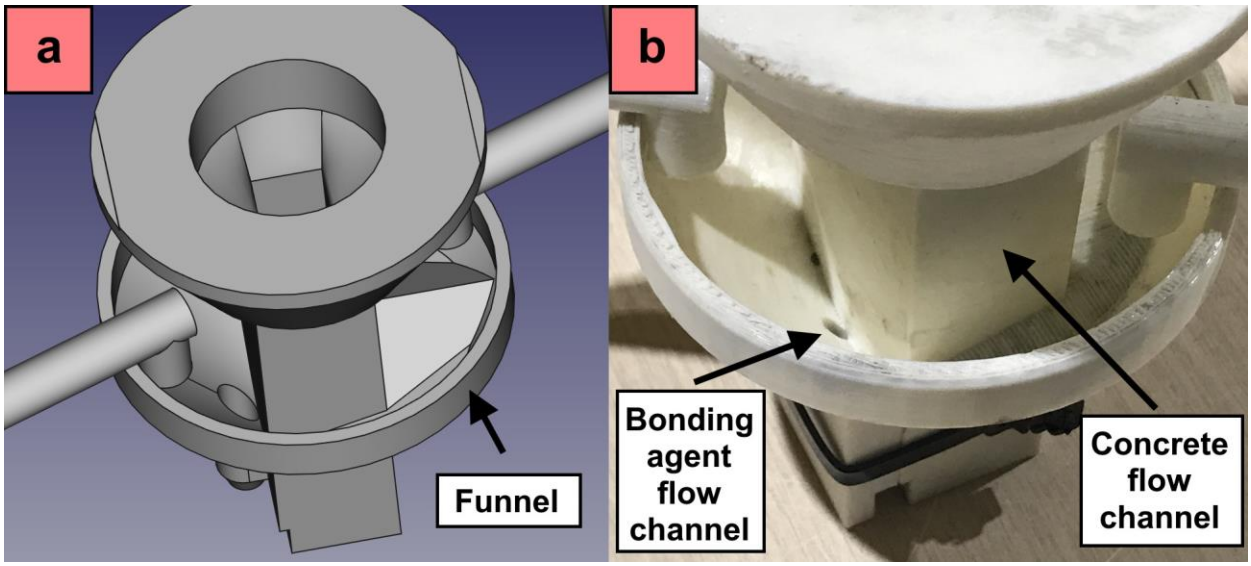


393
394 Fig. 13 The funnel receives bonding agent and delivers it to the bonding agent outlet: (a)
395 CAD drawing; (b) 3D printed polymeric part.
396
397 **5.2. Interlayer surface morphology and materials**
398

In this section, the results of the current work will be discussed for each experiment. All the raw data adopted for analysis are presented in Appendices A and B.

The effects of different bonding agents on the relative bond strength, compared with no bonding agent, are plotted in Fig. 14. As seen in Fig. 14, introducing water between layers reduces the relative bond strength. The samples with water as the bonding agent also have the worst average relative bond strength (78%) among all the samples with different bonding agents. Fig. 15 shows the cross-section of printed specimens manufactured by adding different bonding agents. Compared with Fig. 15(c)-(f), a high porosity can be observed at the cross-section of the interface (Fig. 15(a) and (b)) when the water is used as the bonding agent. The possible reason is that too much water on the interface would clog the pores on the rough surface of the previous layer and, thus, prevent the interaction with the material of the new layer. Consequently, the adherence between the layers reduces [28], and the porosity in the interface increases. As a result, the interlayer bond strength decreases.

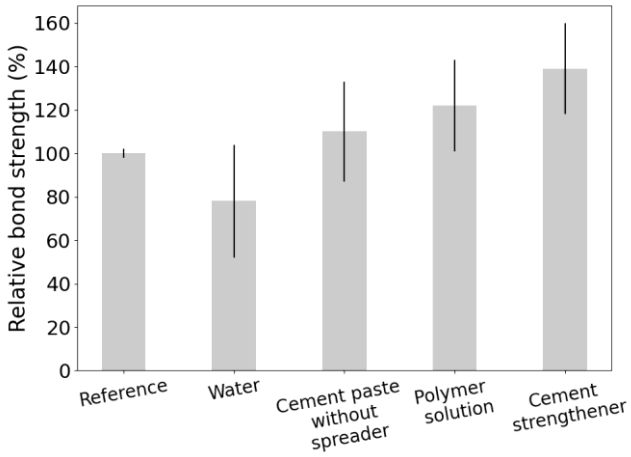


Fig. 14 The effect of different bonding agents on the interlayer bond strength.

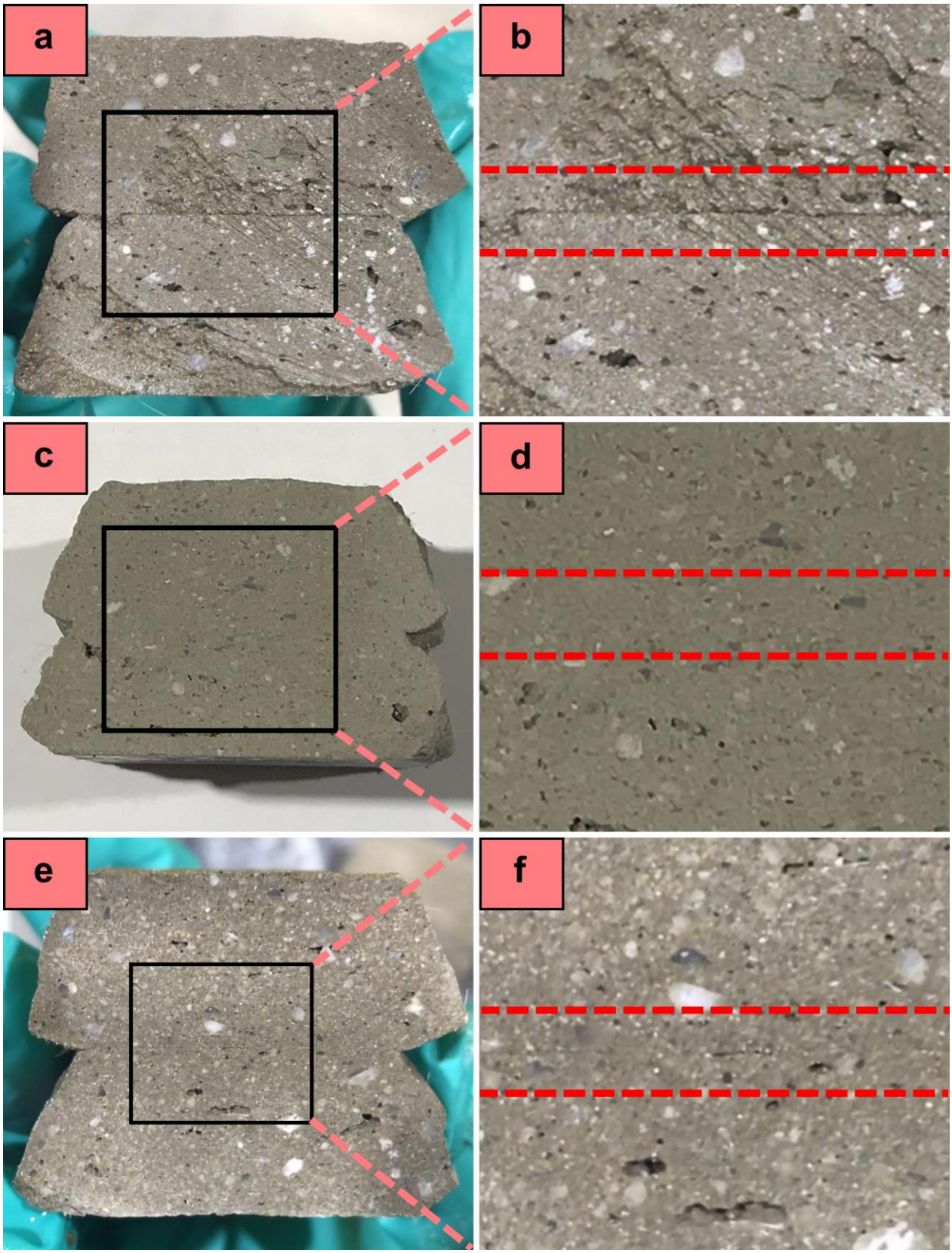


Fig. 15 The cross-section view of the specimens manufactured with different bonding agents: (a) (b) water; (c)(d) polymer solution; (e)(f) cement strengthener.

Moreover, as indicated in Fig. 14, the relative bond strength can reach a higher value when introducing the polymer solution (133%) and the cement strengthener (139%) as bonding agents, which means adding the polymer solution or the cement strengthener between layers can improve the interlayer bond strength. Also, both the polymer solution and cement strengthener produced better interface morphology (Fig. 15(c)-(f)) than water (Fig. 15(a) and (b)). This is attributed to the fact that the polymer can provide extra chemical forces to bond two layers compared to the reference group. For the reference group with no bonding agent, the bond connection can be simply expressed by the interaction of two layers of calcium silicate hydrate (CSH), which has van der Waals forces in the interlayer region. However, adding the sulfur-black-carbon (SBC) polymer between the CSH matrix can introduce different types of forces in the interlayer region, as reported by Hosseini et al. [14]. According to the CSH-SBC-CSH model [14], the interlayer region is filled with electrostatic forces between calcium ions and the negatively-charged SBC polymer. Similar findings were reported by Wang et al. [22], where a polymer-modified mortar was used for interlayer bond strength enhancement.

Cement paste is widely adopted as a high-efficient bonding agent in concrete repairing [21,29,30]. However, while the relative bond strength with the addition of polymer solution and the cement strengthener can reach more than 130%, adding cement paste can only slightly improve the relative bond strength to 110%, as shown in Fig. 14. The possible reason is that the cement paste adopted in this work has a high viscosity and is difficult to flow smoothly after deposited atop the filament surface. Furthermore, the deposited cement paste cannot be spread under the pressure generated by the new layer and finally maintains its formation, as shown in Fig. 16(a). Consequently, additional defects formed at the sides of the deposited cement paste (Fig. 16(b)) deteriorate the interlayer bond strength. As a result, the cement paste cannot effectively act as a bonding agent between layers for interlayer bond strength enhancement.

In order to address the issue associated with the high viscosity of the cement paste, a nozzle with a spreader was designed in this work, and another experiment was conducted to examine the effect of the spreader on interlayer bond strength enhancement.

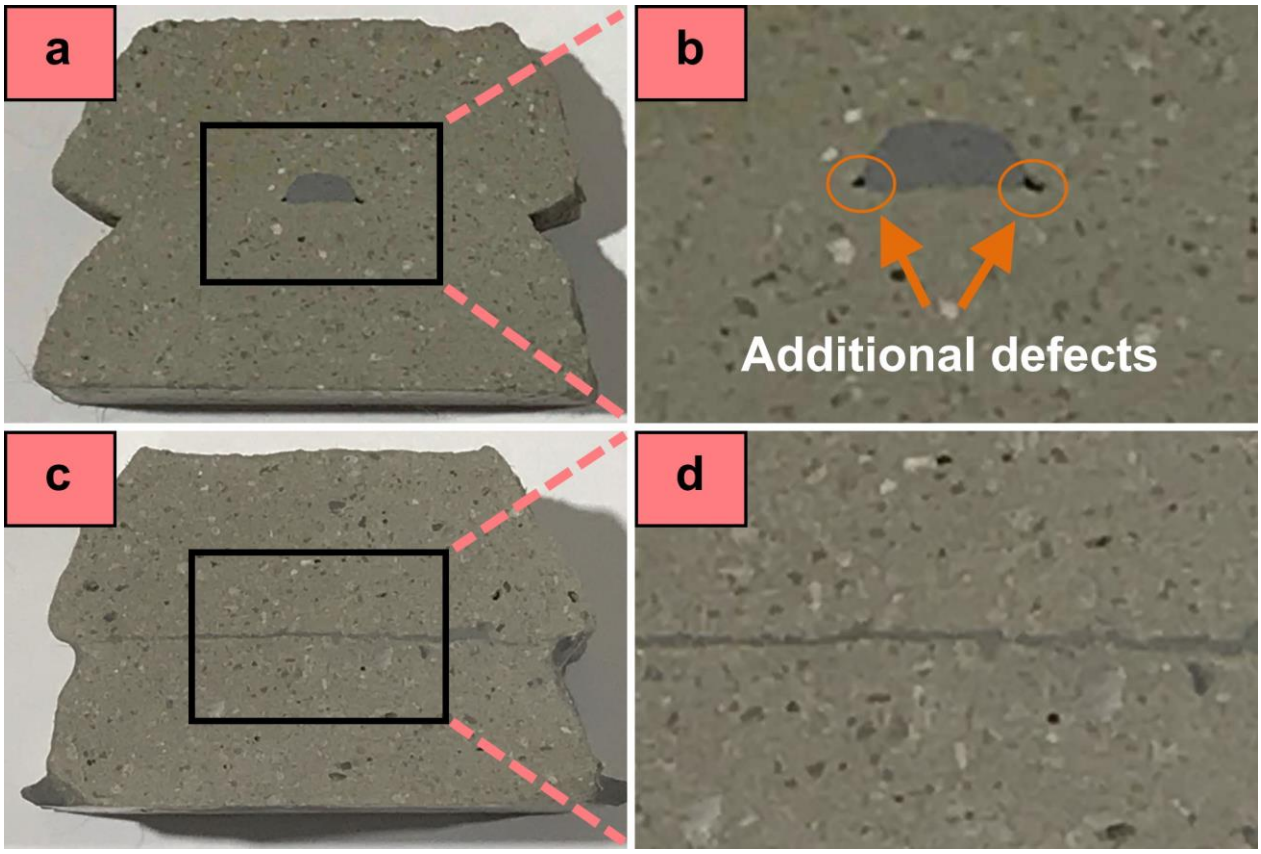


Fig. 16 The cross-section view of the specimens manufactured with cement paste as the bonding agent: (a)(b) by a nozzle without a spreader; (c)(d) by a nozzle with a spreader.

The CAD models and photos of the designed nozzles are shown in Fig. 17. The nozzle shown in Fig. 17(a) and (b) does not have a spreader, while the nozzle shown in Fig. 17(c) and (d) has a spreader attached in the front of the concrete outlet. This spreader is designed to re-disperse the cement paste after the cement paste is deposited atop the printed filament surface during the deposition process. Fig. 16(c) presents the cross-section view of a manufactured specimen by the nozzle with a spreader. Clearly, the cement paste of the specimen shown in Fig. 16(c) is more uniformly distributed between layers compared with that of the specimen shown in Fig. 16(a). Fig. 16(d) shows the zoom-in view of the cross-section, which indicates a better interface with fewer defects than shown in Fig. 16(b). These results prove that the spreader has high efficiency in paving cement paste, a bonding agent with high viscosity, and produces better interlayer bonding strength.

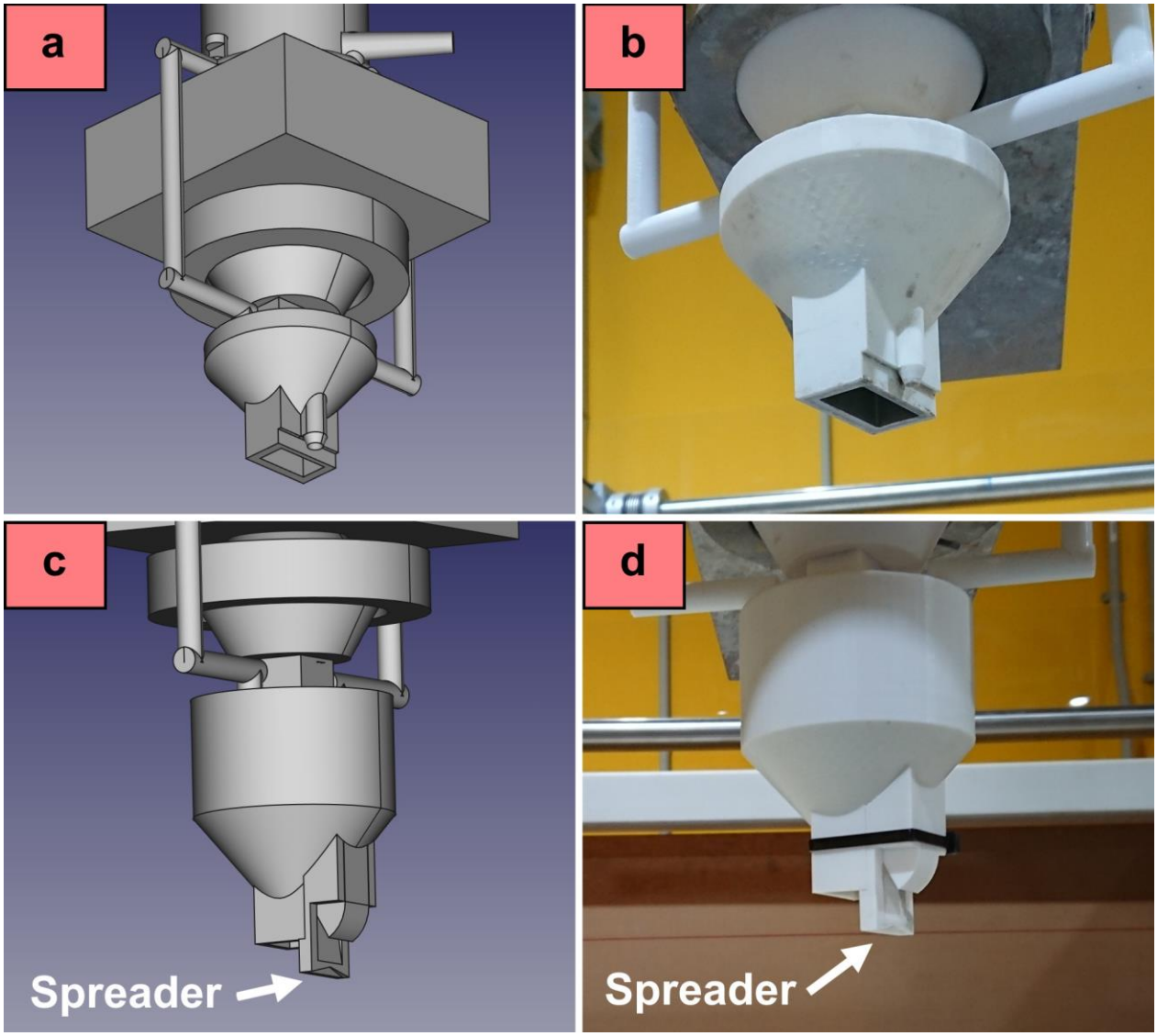


Fig. 17 The designed nozzles: (a) the CAD model of a nozzle without a spreader; (b) a fabricated nozzle without a spreader; (c) the CAD model of a nozzle with a spreader; (d) a fabricated nozzle with a spreader.

The effects of the cement paste with or without a spreader on the interlayer bond strength are plotted in Fig. 18. When the time interval between layers is 40 minutes, the relative bond strength of specimens manufactured by a nozzle with a spreader is higher (267%) than that of specimens manufactured by a nozzle without a spreader (110%). The results reveal that when the cement paste can be dispersed uniformly atop the printed concrete filament, a small amount of cement paste (approximately 500 mL/m$^2$) can be an effective bonding agent for improving the interlayer bond strength.

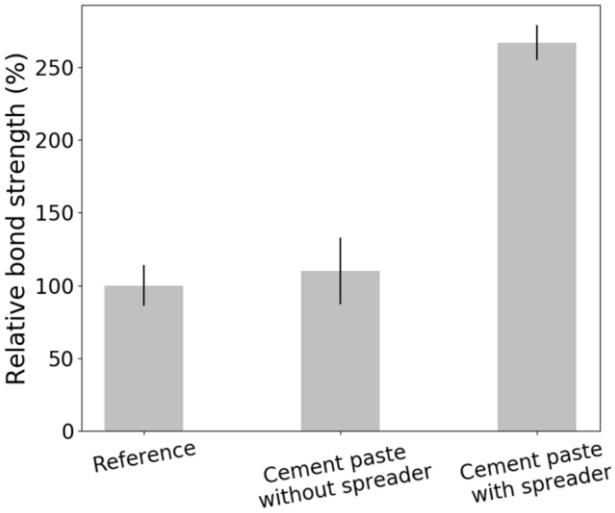


Fig. 18 The effects of the cement paste with or without a spreader on the interlayer bond strength.

### 5.3. Demonstration

In addition to the experimental tests, a demonstration of the concurrent printing and deposition system was also conducted in this work. The demonstration video is included in the supplementary material. To the best of the authors' knowledge, this is the first demonstration showing an automated system to add the bonding agent between layers in the 3DCP process. A designed structure of 600 mm × 500 mm × 210 mm (L × W × H) was continuously printed in 25 minutes, as shown in Fig. 19. The cement strengthener (which is white) was adopted as the bonding agent to obtain better visibility in the demonstration. The successful printing proves that the designed system has great potential for engineering applications.

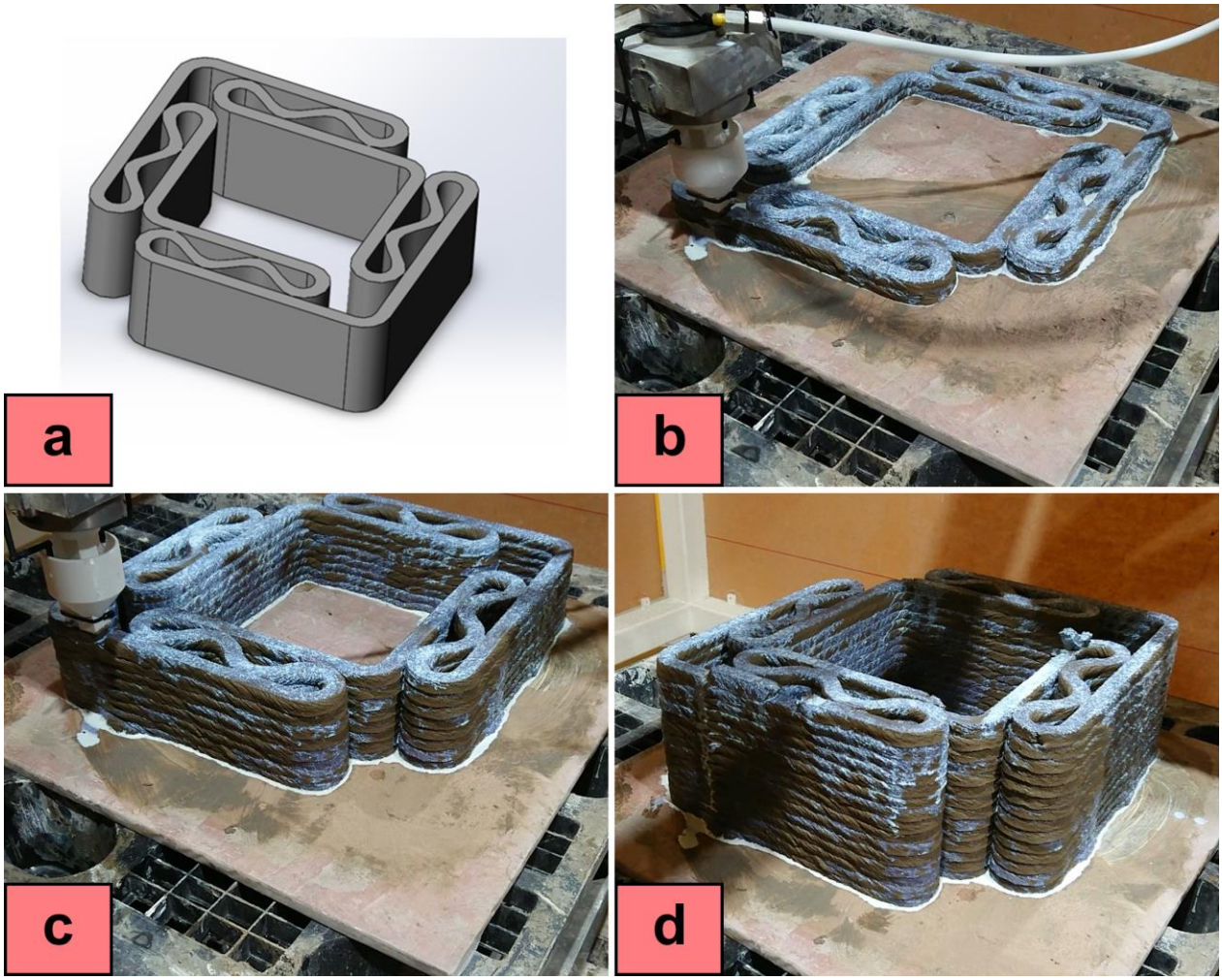


Fig. 19 The demonstration to print a structure of 600 mm × 500 mm × 210 mm (L × W × H) with the presented synchronized concrete and bonding agent deposition system (the demonstration video is included in the supplementary material): (a) the CAD model of the designed structure; (b) The first two layers were printed; (c) The first seven layers were printed; (d) The whole structure was printed.

## 6. Summary, discussion, and future works

### 6.1. Summary and discussion

This study demonstrates a novel synchronized concrete and bonding agent deposition system for interlayer bond strength enhancement in extrusion-based 3DCP. To the best of the authors' knowledge, this is the first time that a concurrent concrete and bonding agent deposition process is presented, proved, and demonstrated. Various bonding agents, including water, a

cement strengthener, a polymer solution, and a cement paste, were tested through controlled experiments. The results indicate that when the time interval between layers is 40 minutes, the relative bond strength compared with no bonding agent can be obtained as high as 267% by using a small amount (approximately 500 mL/m$^2$) of cement paste as the bonding agent. This highlights the importance and efficiency of a concurrent printing and deposition system to enhance the interlayer bond strength. On this basis, the proposed system has contributed to the 3DCP field in the following four aspects:

(1) Safer printed structures. With the combined process of concrete printing and bonding agent deposition, safer structures can be constructed as a result of highly improved interlayer bond strength. By adding bonding agents between layers, the water impermeability of the 3D printed structure may also be improved. These improvements would make 3DCP technology more feasible for the construction industry.

(2) Automation. The synchronized concrete and bonding agent deposition system can be perfectly compatible with 3DCP and fabricate 3D printed structure with admirable interlayer bond strength. Compared with other bonding improving methods in previous literature, the presented system can deposit the bonding agent concurrently and automatically with the concrete printing process, and the resulted efficiency makes the system more practicable for future digital concrete applications.

(3) Lower application barriers. The decreased interlayer bond strength with large interlayer time intervals sets high requirements for 3DCP to meet application requirements. To address such a limitation, it is usually necessary to modify the material design, better plan the printing path, or adopt higher-end printers. However, the proposed system makes the limitation less critical and would potentially lower the barriers and widen the applications of 3DCP.

(4) New thinking. The synchronized system improves 3D printed structure performance from a brand-new perspective. Instead of focusing on the 3D printable materials, the proposed system improves the interlayer bond strength by the design of print-head and process. Furthermore, similar thinking and systems could be applied for the construction of other functional components by simultaneously depositing multiple

materials (e.g., cementitious materials, sand powder, ceramic, and other functional materials).

### 6.2. Future works

With the demonstration of the synchronized concrete and bonding agent deposition system for interlayer bond strength enhancement, the primary future is to integrate and coordinate the sub-systems to boost digital concrete automation to a greater extent. Additionally, further research will focus on the effects on the interface microstructure of different bonding agents with various time intervals. Since the interface microstructure decides many properties of 3D printed concrete structure, this investigation will help to explain different bonding performances and optimize the concurrent deposition process.

Apart from the microstructural investigation, bonding agents for different interface enhancement purposes (e.g., improving water impermeability and durability) in digital concrete will be screened. The exploration of functional interface properties by adding functional agents, such as self-healing agents and self-sensing agents, is also of great research interest.

## Declaration of competing interest

The authors declare no conflict of interest.

## Credit authorship contribution statement

**Yiwei Weng**: Conceptualization, Methodology, Investigation, Data curation, Formal analysis, Validating, Writing - original draft, review & editing

**Mingyang Li:** Supervision, Conceptualization, Methodology, Investigation, Data curation, Formal analysis, Validating, Writing - original draft, review & editing

**Teck Neng Wong:** Supervision, Funding acquisition, Writing - review & editing.

**Ming Jen Tan:** Supervision, Funding acquisition, Writing - review & editing.

## Acknowledgments

The authors would like to acknowledge National Research Foundation, Prime Minister's Office, Singapore under its Medium-Sized Centre funding scheme, Singapore Centre for 3D Printing, CES_SDC Pte Ltd, and Chip Eng Seng Corporation Ltd for their funding and support in this research project.

## Appendix A: The raw data of the splitting tensile tests of the specimens manufactured with various bonding agents

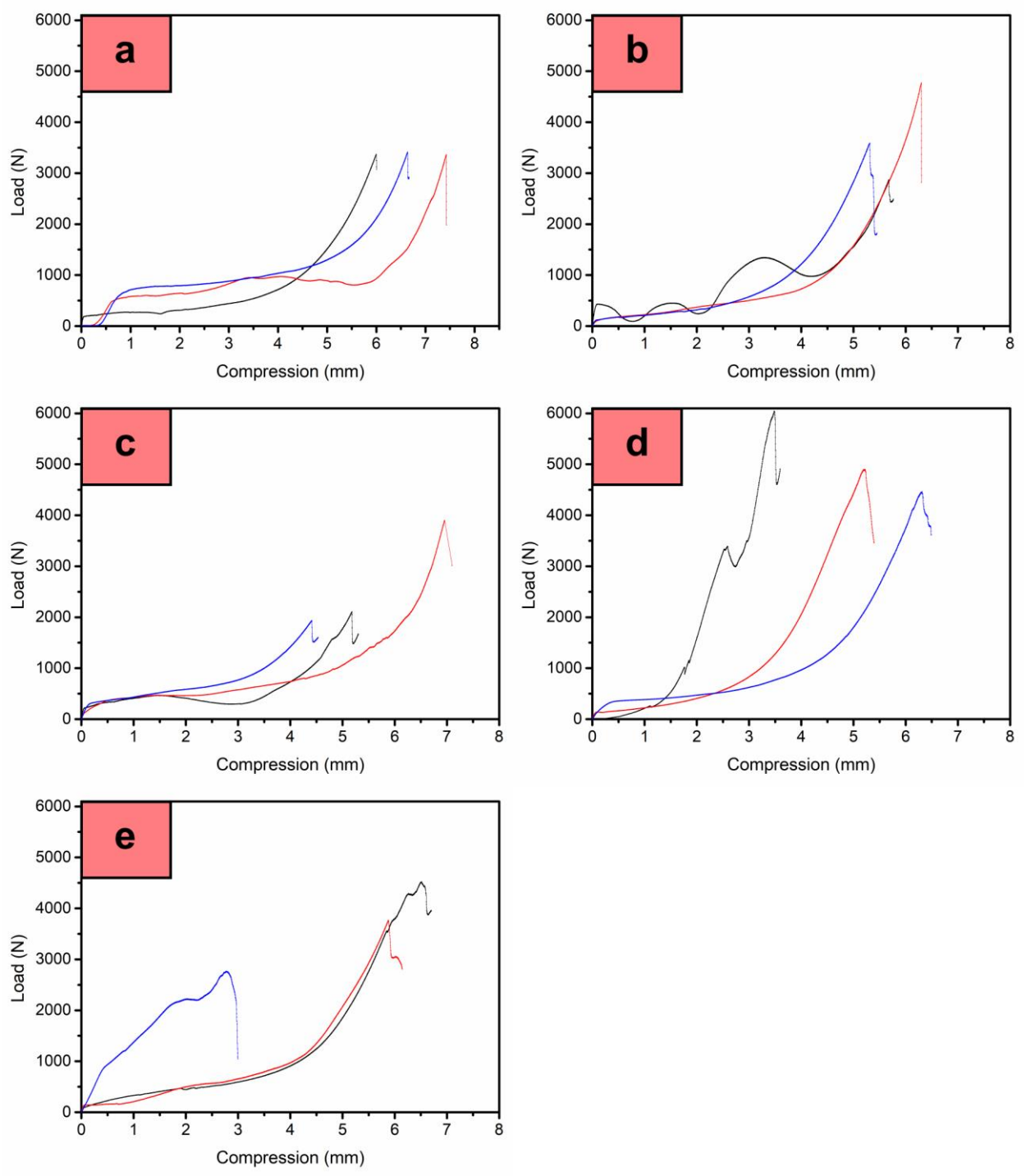


Fig. A1 The splitting tensile test results of the specimens manufactured with various bonding agents: (a) no bonding agent (reference group); (b) cement paste; (c) water; (d) cement strengthener; (e) polymer solution.

## Appendix B: The raw data of the splitting tensile tests of the specimens manufactured with or without the spreader

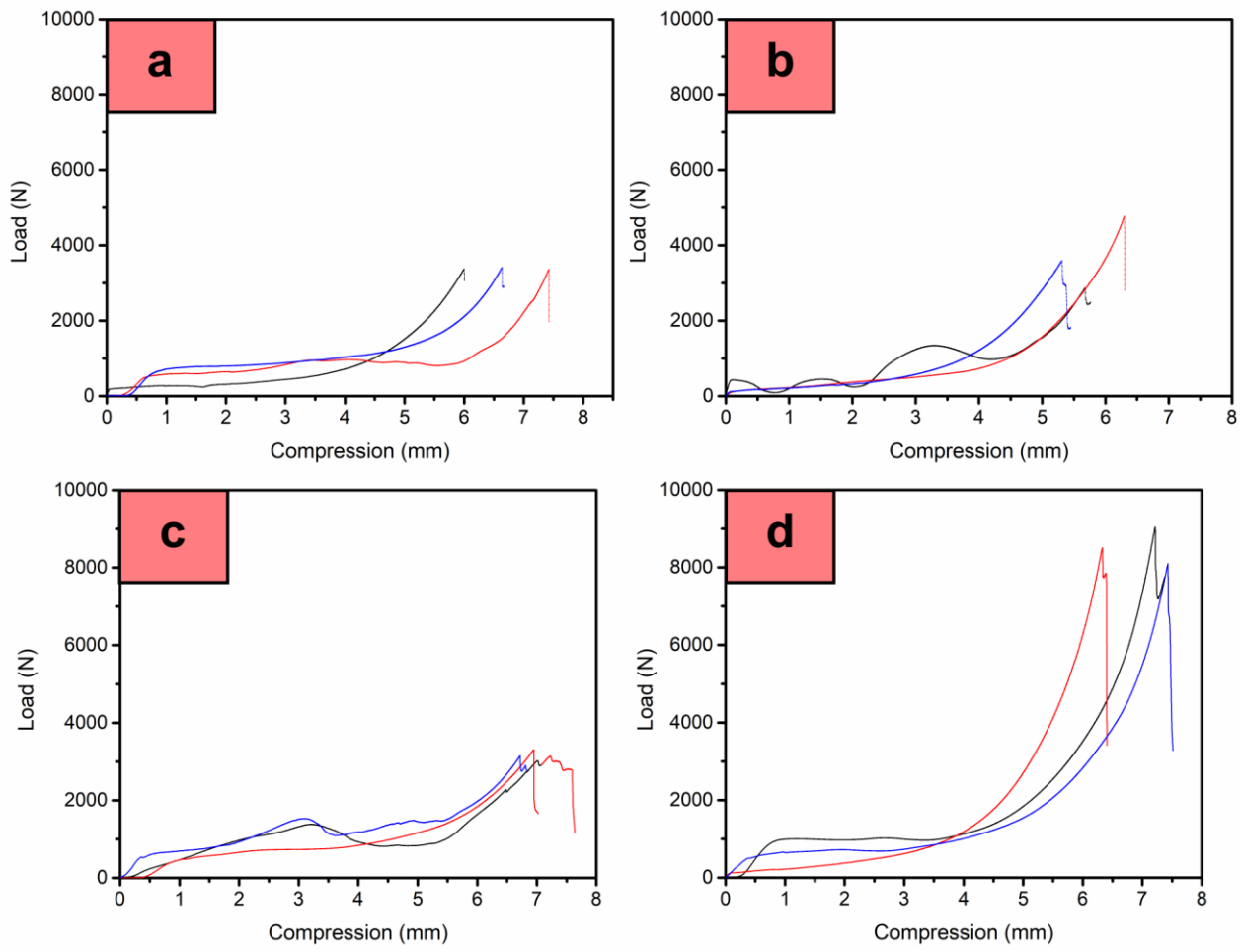


Fig. B1 The splitting tensile test results of the specimens manufactured: (a) with no bonding agent (reference group) by a nozzle without a spreader (Fig. A1(a)); (b) with cement paste as the bonding agent by a nozzle without a spreader (Fig. A1(b)); (c) with no bonding agent (reference group) by a nozzle with a spreader; (d) with cement paste as the bonding agent by a nozzle with a spreader.

## References

[1] B. García de Soto, I. Agustí-Juan, J. Hunhevicz, S. Joss, K. Graser, G. Habert, B.T. Adey,

Productivity of digital fabrication in construction: Cost and time analysis of a robotically built wall, Automation in Construction. 92 (2018) pp. 297–311. https://doi.org/10.1016/j.autcon.2018.04.004.

[2] I. Agustí-juan, F. Müller, N. Hack, T. Wangler, G. Habert, Potential benefits of digital fabrication for complex structures : Environmental assessment of a robotically fabricated concrete wall, Journal of Cleaner Production. 154 (2017) pp. 330–340. https://doi.org/10.1016/j.jclepro.2017.04.002.

[3] Y. Weng, M. Li, M.J. Tan, S. Qian, M. Jen, S. Qian, M.J. Tan, S. Qian, Design 3D printing cementitious materials via Fuller Thompson theory and Marson-Percy model, Construction and Building Materials. 163 (2018) pp. 600–610. https://doi.org/10.1016/j.conbuildmat.2017.12.112.

[4] V. Mechtcherine, V.N. Nerella, F. Will, M. Näther, J. Otto, M. Krause, Large-scale digital concrete construction – CONPrint3D concept for on-site, monolithic 3D-printing, Automation in Construction. 107 (2019) pp. 102933. https://doi.org/10.1016/j.autcon.2019.102933.

[5] Y. Weng, M. Li, M.J. Tan, S. Qian, 3D Printable high performance fiber reinforced cementitious composites for large-scale printing, Proceedings of the 3rd International Conference on Progress in Additive Manufacturing (Pro-AM 2018). (2018) pp. 19–24. https://doi.org/10.25341/D4B591.

[6] Y. Weng, M. Li, S. Ruan, T.N. Wong, M.J. Tan, K. Leong, O. Yeong, S. Qian, Comparative economic, environmental and productivity assessment of a concrete bathroom unit fabricated through 3D printing and a precast approach, Journal of Cleaner Production. 261 (2020) pp. 121245. https://doi.org/10.1016/j.jclepro.2020.121245.

[7] E. Keita, H. Bessaies-bey, W. Zuo, P. Belin, N. Roussel, Weak bond strength between successive layers in extrusion-based additive manufacturing: measurement and physical origin, Cement and Concrete Research. 123 (2019) pp. 105787. https://doi.org/10.1016/j.cemconres.2019.105787.

[8] G. De Schutter, K. Lesage, V. Mechtcherine, V.N. Nerella, G. Habert, I. Agusti-Juan, Vision of 3D printing with concrete — Technical, economic and environmental potentials, Cement and Concrete Research. 112 (2018) pp. 25–36. https://doi.org/10.1016/j.cemconres.2018.06.001.

[9] R. Buswell, W.R. Silva, J. S.Z., J. Dirrenberger, 3D printing using concrete extrusion: a roadmap for research, Cement and Concrete Research. 112 (2018) pp. 37–49. https://doi.org/10.1016/j.cemconres.2018.05.006.

[10] T. Marchment, J. Sanjayan, Mesh reinforcing method for 3D Concrete Printing, Automation in Construction. 109 (2020) pp. 102992. https://doi.org/10.1016/j.autcon.2019.102992.

[11] B. Lu, Y. Weng, M. Li, Y. Qian, K.F. Leong, M.J. Tan, S. Qian, A systematical review of 3D printable cementitious materials, Construction and Building Materials. 207 (2019) pp. 477–490. https://doi.org/10.1016/j.conbuildmat.2019.02.144.

[12] G. Ma, Z. Li, L. Wang, Printable properties of cementitious material containing copper tailings for extrusion based 3D printing, Construction and Building Materials. 162 (2018) pp. 613–627. https://doi.org/10.1016/j.conbuildmat.2017.12.051.

[13] B. Zareiuam, B. Khonshnevis, Effect of interlocking on interlayer adhesion and strength of structures in 3D printing of concrete, Automation in Construction. 83 (2017) pp. 212–221. https://doi.org/10.1016/j.autcon.2017.08.019.

[14] E. Hosseini, M. Zakertabrizi, A.H. Korayem, G. Xu, A novel method to enhance the interlayer bonding of 3D printing concrete An experimental and computational investigation, Cement and Concrete Composites. 99 (2019) pp. 112–119. https://doi.org/10.1016/j.cemconcomp.2019.03.008.

[15] T.T. Le, S.A. Austin, S. Lim, R.A. Buswell, R. Law, A.G.F. Gibb, T. Thorpe, Hardened properties of high-performance printing concrete, Cement and Concrete Research. 42 (2012) pp. 558–566. https://doi.org/10.1016/j.cemconres.2011.12.003.
[16] R.J.M. Wolfs, F.P. Bos, T.A.M. Salet, Hardened properties of 3D printed concrete: The influence of process parameters on interlayer adhesion, Cement and Concrete Research. 119 (2019) pp. 132–140. https://doi.org/10.1016/j.cemconres.2019.02.017.
[17] M. Xia, B. Nematollahi, J. Sanjayan, Printability, accuracy and strength of geopolymer made using powder-based 3D printing for construction applications, Automation in Construction. 101 (2019) pp. 179–189. https://doi.org/10.1016/j.autcon.2019.01.013.
[18] M. Xia, J. Sanjayan, Method of formulating geopolymer for 3D printing for construction applications, Materials and Design. 110 (2016) pp. 382–390. https://doi.org/10.1016/j.matdes.2016.07.136.
[19] G. Ma, Z. Li, L. Wang, F. Wang, J. Sanjayan, Mechanical anisotropy of aligned fiber reinforced composite for extrusion-based 3D printing, Construction and Building Materials. 202 (2019) pp. 770–783. https://doi.org/10.1016/j.conbuildmat.2019.01.008.
[20] J.G. Sanjayan, M. Xia, Effect of Surface Moisture on Inter-Layer Strength of 3D Printed Concrete, Construction and Building Materials. 172 (2018) pp. 468–475. https://doi.org/10.1016/j.conbuildmat.2018.03.232.
[21] Q. Yang, B. Zhu, S. Zhang, X. Wu, Properties and applications of magnesia-phosphate cement mortar for rapid repair of concrete, Cement and Concrete Research. 30 (2000) pp. 1807–1813. https://doi.org/10.1016/S0008-8846(00)00419-1.
[22] L. Wang, Z. Tian, G. Ma, M. Zhang, Interlayer bonding improvement of 3D printed concrete with polymer modified mortar: experiments and molecular dynamics studies, Cement and Concrete Composites. 110 (2020) pp. 103571. https://doi.org/10.1016/j.cemconcomp.2020.103571.
[23] T. Marchment, J. Sanjaan, M. Xia, Method of enhancing interlayer bond strength in construction scale 3D printing with mortar by effective bond area amplification, Materials and Design. 169 (2019) pp. 107684. https://doi.org/10.1016/j.matdes.2019.107684.
[24] Y. Weng, M. Li, Z. Liu, B. Lu, D. Zhang, M.J. Tan, Printability and fire performance of a developed 3D printable fibre reinforced cementitious composites under elevated temperatures, Virtual and Physical Prototyping. 14 (2019) pp. 284–292. https://doi.org/10.1080/17452759.2018.1555046.
[25] ASTM C496 / C496M - 17, Standard Test Method for Splitting Tensile Strength of Cylindrical Concrete Specimens, ASTM International, West Conshohocken, PA. (2017). https://doi.org/10.1520/C0496.
[26] K. Rashid, T. Ueda, D. Zhang, K. Miyaguchi, H. Nakai, Experimental and analytical investigations on the behavior of interface between concrete and polymer cement mortar under hygrothermal conditions, Construction and Building Materials. 94 (2015) pp. 414–425. https://doi.org/10.1016/j.conbuildmat.2015.07.035.
[27] B. Zareiyan, B. Khoshnevis, Interlayer adhesion and strength of structures in Contour Crafting - Effects of aggregate size, extrusion rate, and layer thickness, Automation in Construction. 81 (2017) pp. 112–121. https://doi.org/10.1016/j.autcon.2017.06.013.
[28] D.P. Bentz, I. De la Varga, J.F. Muñoz, R.P. Spragg, B.A. Graybeal, D.S. Hussey, D.L. Jacobson, S.Z. Jones, J.M. LaManna, Influence of substrate moisture state and roughness on interface microstructure and bond strength: Slant shear vs. pull-off testing, Cement and Concrete Composites. 87 (2018) pp. 63–72. https://doi.org/10.1016/j.cemconcomp.2017.12.005.
[29] G. Xiong, J. Liu, G. Li, H. Xie, A way for improving interfacial transition zone between concrete substrate and repair materials, Cement and Concrete Research. 32 (2002) pp.

715 1877–1881. https://doi.org/10.1016/S0008-8846(02)00840-2.
716 [30] G. Li, H. Xie, G. Xiong, Transition zone studies of new-to-old concrete with different
717 binders, Cement and Concrete Composites. 23 (2001) pp. 381–387.
718 https://doi.org/10.1016/S0958-9465(01)00002-6.
719